Journal of Science and Technology in Civil Engineering NUCE 2019. 13 (2): 1–11

FREE-VIBRATION ANALYSIS OF MULTI-DIRECTIONAL FUNCTIONALLY GRADED PLATES BASED ON 3D ISOGEOMETRIC ANALYSIS

Thai Son[a,*], Thai Huu Tai[a]

[a]*Department of Infrastructure Engineering, The University of Melbourne, Parkville, VIC 3010, Australia*

Article history:
Received 04/03/2019, Revised 18/03/2019, Accepted 19/04/2019

Abstract

In this paper, an efficient computational approach is developed to investigate the free-vibration behavior of functionally graded plates. The problem is developed based on a three-dimensional elasticity theory, which is expected to capture the structural response accurately. Isogeometric analysis is employed as a discretion tool to solve the problems. The accuracy of the proposed approach is verified by comparing the obtained results with those available in the literature. In addition, various examples are also presented to illustrate the efficiency of the proposed approach. There are five types of plates with different configurations of material gradations. The benchmark results for those are also given for future investigations.

Keywords: multi-directional functionally graded materials; 3D elasticity; isogeometric analysis; free-vibration.

https://doi.org/10.31814/stce.nuce2019-13(2)-01

1. Introduction

In the field of engineering structures, macroscopically inhomogeneous materials are widely employed for practical applications [1]. One of those materials is laminated composites, whose material properties are piecewise constant in the thickness through the thickness of structures. In mechanical perspective, the use of laminated composite is susceptible to locally failure. This is due to the effect of discontinuous distribution of material properties in the interfaces between laminate, which could result in a locally large plastic deformation and micro-crack propagation. The adverse features of traditional laminated composite materials are eliminated in a different class of composite materials, which is termed Functionally Graded Materials (FGMs) and dates back to the pioneer studies by Koizumi [2, 3]. FGMs are widely considered as spatial composites, in which the gradual changes of volume fractions of the constituent materials in defined directions results in a smooth transition of material properties. Normally, FGMs are made from two distinct material constituents (ceramic and metal constituents). The combination of these materials results in a new type of composite material that inherits the preferable features of both, such as high-ductility and high-thermal resistance. Thanks to this feature, FGMs are now widely applied in various industrial fields such as aerospace, piezoelectric sensor, nuclear plants and etc.

As indicated in a review study [4], the majority of previous studies on Functionally Graded (FG) plates only focused on those made from uni-directional FGMs. However, it was also pointed out by

*Corresponding author. *E-mail address:* son.thai@unimelb.edu.au (Son, T.)

Nemat-Alla [5] that the use of uni-directional FGMs might not be effective when the structures are exposed to severe conditions, especially in the case of thermal problems. Therefore, it is necessary to investigate for a more complex variation of material constituents in FGMs besides thickness gradations. This requirement might results in a new class of multi-directional FGMs, however, that the studies for multi-directional FGMs are rare in the literature. Lü et al. [6] used the state space approach to conduct a semi-analytical analysis on the static behavior of multi-directional FG plates. Nie and Zhong [7] also employed a similar semi-analytical approach to investigate the dynamic problems of multi-directional FG annular plates. The free-vibration behavior of multi-directional FG circular plates resting on elastic foundations was also examined by Shariyat and Alipour [8]. The authors employed the differential transformation method to obtain a semi-analytical solution for the problem. The multi-directional FGMs were also investigated for the thin-wall structures in [9, 10]. Recently, Wang et al. [11] also presented a study on the free-vibration analysis of 3D multi-directional FG plate, where the solutions are derived based on the quadrature element method. Overall, it is seen that the solutions for the problems of multi-directional FG plates are not easy to obtained from an analytical approach. This is due to the fact that the gradation of materials in spatial form requires a considerable amount of computational effort. In addition, the use of simplified 2D plates theories might not capture all the behavior of a plate for the case of multi-directional FGMs [11]. Therefore, rigorous 3D elastic solutions should be derived to be used as benchmark results for other studies, where simplified models are used.

Isogeometric Analysis proposed by Hughes et al. [12] is widely considered as an advanced Finite Element Method (FEM) that bridges the gap between CAD technologies and finite element method. Since it was first introduced in 2005, the IGA has been widely developed to deal with computational problems in different engineering fields [13]. In general, the IGA brings two prominent advantages that are superior to traditional finite element methods. The first preferable feature comes from the fact that the CAD tools are employed in the IGA approach, hence geometries with curves and elliptical shapes are modeled accurately in the analysis model. The remaining feature is that the NURBS functions in IGA can provide high-continuous interpolation, which is not straightforward in a traditional finite element approach. This feature is supported by an advanced technique called k-refinement scheme, which is considered as a combination of h- and p-refinement schemes in traditional FEM and is able to reduce the degree of freedoms for high-order elements. The efficiency of this approach on the analysis of unidirectional FG 3D plates was addressed in the study of Nguyen and Nguyen-Xuan [14]. In addition, the IGA-based models were also successfully developed to deal with optimization problems of multi-directional FG plates by Lieu-Xuan and his colleagues [15–18].

In this study, the advanced features of IGA approach are employed to study the free-vibration problems of multi-directional FG plates. The governing equations for the general 3D elastic solutions are derived based on the virtual energy approach. NURBS basis functions from IGA approach are employed as interpolations of geometric and displacement variables. Various numerical examples of different plates' geometries and material gradations area also presented to show the efficiency of the approach. The solutions for multi-directional FG plates in this study could be considered as benchmark results for further investigations.

2. Formulation of the 3D elasticity problem

Consider an elastic body in the Cartesian coordinate system, the constitutive equation and stress-strain relations in case of infinitesimal strain problems are expressed as follows

$$\sigma_{ij} = 2\mu\varepsilon_{ij} + \lambda\varepsilon_{kk}\delta_{ij} \tag{1}$$

$$\varepsilon_{ij} = \frac{1}{2}\left(u_{i,j} + u_{j,i}\right) \tag{2}$$

where σ_{ij} is the stress tensor, ε_{ij} is the strain tensor, u_i is the displacement of a point, δ_{ij} is the Kronecker delta, μ and λ are Lame's constant. The virtual strain energy and kinetic energy stored in an elastic body having volume Ω are given by

$$\delta U = \int_{\Omega} \sigma_{ij}\delta\varepsilon_{ij} d\Omega \tag{3}$$

$$\delta T = -\int_{\Omega} \rho\ddot{u}_i\delta u_i d\Omega \tag{4}$$

where ρ is the mass density. The governing equation is obtained according to the principle of virtual energy as follows

$$\int_{\Omega} \left(\sigma_{ij}\delta\varepsilon_{ij} + \rho\ddot{u}_i\delta u_i\right) d\Omega = 0 \tag{5}$$

The double dot in Eq. (5) denotes the second derivative with respect to time t.

3. IGA-Based finite element formulations

3.1. A brief review of IGA and its elements

In the concept of IGA approach, a knot vector is fundamental component. It is a non-decreasing coordinate in parameter space.

$$\Xi = \left\{\xi_1, \xi_2, \xi_3, ..., \xi_i, ..., \xi_{n+p+1}\right\}, \quad \xi_i \leq \xi_{i+1} \tag{6}$$

where ξ_i is the i^{th} knot, n is the number of knot function, and p is the order of B-spline basis function. For a given knot, the formulation of B-spline basic functions are recursively starting with $p = 0$

$$N_{i,0}(\xi) = \begin{cases} 1 & \xi_i \leq \xi < \xi_{i+1} \\ 0 & \text{otherwise} \end{cases} \tag{7}$$

and for $p \geq 1$

$$N_{i,p} = \frac{\xi - \xi_i}{\xi_{i+p} - \xi_i} N_{i,p-1}(\xi) + \frac{\xi_{i+p+1} - \xi}{\xi_{i+p+1} - \xi_{i+1}} N_{i,p-1}(\xi) \tag{8}$$

It is noted herein that the fraction 0/0 is assumed to be zero. The univariable NURBS basic functions are constructed based on B-spline functions with a set of weight as follows

$$R_i^p(\xi) = \frac{N_{i,p}(\xi) w_i}{W(\xi)} = \frac{N_{i,p}(\xi) w_i}{\sum_{\hat{i}=1}^{n} N_{\hat{i},p}(\xi) w_{\hat{i}}} \tag{9}$$

in which w_i is the weight value. The multivariate NURBS basic functions are defined based on the tensor product

$$R_{i,j,k}^{p,q,r}(\xi,\eta,\zeta) = \frac{N_{i,p}(\xi) M_{i,q}(\eta) L_{k,r}(\zeta) w_{i,j,k}}{\sum_{\hat{i}=1}^{n}\sum_{\hat{j}=1}^{m}\sum_{\hat{k}=1}^{k} N_{\hat{i},p}(\xi) M_{\hat{j},q}(\eta) L_{\hat{k},r}(\zeta) w_{\hat{i},\hat{j},\hat{k}}} \tag{10}$$

To define a 3D NURBS geometry, the NUBRS functions are combined with the associated control points in a linear combination as follows

$$\Omega(\xi,\eta,\zeta) = \sum_{\hat{i}=1}^{n}\sum_{\hat{j}=1}^{m}\sum_{\hat{k}=1}^{k} R_{i,j,k}^{p,q,r}(\xi,\eta,\zeta)\mathbf{B}_{i,j,k} \tag{11}$$

3.2. NURBS-based formulation for 3D elasticity problem

By using the NURBS basic functions as interpolations, the displacement variables can be expressed as follows

$$\mathbf{u} = \sum_{i=1}^{n} R_i \mathbf{d}_i \tag{12}$$

where $\mathbf{u} = \begin{Bmatrix} u_1 & u_2 & u_3 \end{Bmatrix}^T$ is the displacement variable and $\mathbf{d} = \begin{Bmatrix} u_{c1} & u_{c2} & u_{c3} \end{Bmatrix}^T$ is the degrees of freedom associated with a control point, R is the interpolation function. The strain tensor can be written as follows

$$\boldsymbol{\varepsilon} = \begin{Bmatrix} \varepsilon_{xx} \\ \varepsilon_{yy} \\ \varepsilon_{zz} \\ \gamma_{yz} \\ \gamma_{xz} \\ \gamma_{xy} \end{Bmatrix} = \begin{bmatrix} R_{,x} & 0 & 0 \\ 0 & R_{,y} & 0 \\ 0 & 0 & R_{,z} \\ 0 & R_{,z} & R_{,y} \\ R_{,z} & 0 & R_{,x} \\ R_{,y} & R_{,x} & 0 \end{bmatrix} \begin{Bmatrix} u_1 \\ u_2 \\ u_3 \end{Bmatrix} = \mathbf{B}_{\varepsilon} \mathbf{d} \tag{13}$$

The stress tensor can be expressed in matrix form as

$$\boldsymbol{\sigma} = \begin{Bmatrix} \sigma_x \\ \sigma_y \\ \sigma_z \\ \sigma_{yz} \\ \sigma_{xz} \\ \sigma_{xy} \end{Bmatrix} = \begin{bmatrix} Q_{11} & Q_{12} & Q_{13} & 0 & 0 & 0 \\ Q_{12} & Q_{22} & Q_{23} & 0 & 0 & 0 \\ Q_{13} & Q_{23} & Q_{33} & 0 & 0 & 0 \\ 0 & 0 & 0 & Q_{44} & 0 & 0 \\ 0 & 0 & 0 & 0 & Q_{55} & 0 \\ 0 & 0 & 0 & 0 & 0 & Q_{66} \end{bmatrix} \begin{Bmatrix} \varepsilon_x \\ \varepsilon_y \\ \varepsilon_z \\ \gamma_{yz} \\ \gamma_{xz} \\ \gamma_{xy} \end{Bmatrix} = \mathbf{C}\boldsymbol{\varepsilon} \tag{14}$$

where

$$Q_{11} = Q_{22} = Q_{33} = \frac{E(1-\nu)}{(1+\nu)(1-2\nu)} \tag{15}$$

$$Q_{12} = Q_{13} = Q_{23} = \frac{\nu E}{(1+\nu)(1-2\nu)} \tag{16}$$

$$Q_{44} = Q_{55} = Q_{66} = \frac{E}{2(1+\nu)} \tag{17}$$

It is noted that the values of elastic modulus E, Poisson's ratio ν and the mass density ρ are the spatial functions of locations (x, y, z). The effective values of those material properties are calculated as follows

$$E(x, y, z) = (E_c - E_m) V_c + E_m \tag{18}$$

$$\nu(x, y, z) = (\nu_c - \nu_m) V_c + \nu_m \tag{19}$$

$$\rho(x, y, z) = (\rho_c - \rho_m) V_c + \rho_m \tag{20}$$

where the subscript m and c indicate the properties of metal and ceramic constituents, respectively. V_c is the volume fraction of ceramic constituent and is defined based on a pre-defined distribution law. By substituting Eqs. (13) and (14) into Eq. (5), the governing equation can be rewritten as

$$\int_{\Omega} \left(\delta \mathbf{d}^T \mathbf{B}_{\varepsilon}^T \mathbf{C} \mathbf{B}_{\varepsilon} \mathbf{d} + \rho \delta \mathbf{d}^T \mathbf{R}_u^T \mathbf{R}_u \ddot{\mathbf{d}} \right) d\Omega \tag{21}$$

Then, the system equation of IGA-based finite element model can be rewritten as

$$\left(\mathbf{K} - \omega^2 \mathbf{M}\right)\mathbf{d} = \mathbf{0} \tag{22}$$

where the stiffness matrix $\mathbf{K}$ and the mass matrix $\mathbf{M}$ are given by

$$\mathbf{K} = \int_{\Omega} \mathbf{B}_{\varepsilon}^{T} \mathbf{C} \mathbf{B}_{\varepsilon} d\Omega \tag{23}$$

$$\mathbf{M} = \int_{\Omega} \rho \mathbf{R}_{u}^{T} \mathbf{R}_{u} d\Omega \tag{24}$$

in which

$$\mathbf{R}_{u} = \begin{bmatrix} R & 0 & 0 \\ 0 & R & 0 \\ 0 & 0 & R \end{bmatrix} \tag{25}$$

4. Numerical examples

In this section, the verification study is firstly conducted to validate the accuracy and efficiency of the present approach to the free-vibration analysis of multi-directional FG plates. Then, various numerical examples on the free-vibration responses of multi-directional FG plates with different shapes and geometries are also presented. Different types of material gradations are also taken into account. The results obtained from this subsection could be used as benchmark results for further investigation.

4.1. Verification and convergence studies

In this study, an Al/ZrO_2-2 square plate addressed in the study of Hosseini-Hashemi et al. [19] is revisited. The material properties of Al (metal) are $E = 70$ GPa, $\nu = 0.3$, $\rho = 2707$ kg/m^3, and those for ZrO_2-2 (ceramic) are $E = 168$ GPa, $\nu = 0.3$, $\rho = 5700$ kg/m^3. The constituents of the materials in the plate is assumed to vary in the thickness direction with the distribution law of the volume fraction of ceramic constituent is given as follows

$$V_c = \left(\frac{1}{2} - \frac{z}{h}\right)^n \tag{26}$$

where h is the thickness of the plate and $h/a = 0.05$. The boundary condition for this example is SCSF, where S and C stand for simply supported boundary and clamped boundary, respectively. In case of a rectangular plate, the simply supported boundary condition is given by

$$\begin{aligned} u_2 = u_3 = 0 \ \text{ at } \ x = 0, a \\ u_1 = u_3 = 0 \ \text{ at } \ y = 0, b \end{aligned} \tag{27}$$

and the clamped boundary condition is given by

$$u_2 = u_3 = u_3 = 0 \tag{28}$$

where a and b are the side length of the plate. It is noted that the origin of the coordinate is located in the middle plane of the plate. Table 1 compares the results obtained from this study and the exact

solutions given by Hosseini-Hashemi et al. [19], where $\bar{\omega} = \omega\left(a^2/h\right)\sqrt{\rho_M/E_M}$. Overall, it is seen that the present results are in good agreement with those provided in the referenced study. In addition, it is seen that the convergence rate is faster with higher order p. Good convergence solutions are obtained with $p = 3$ and the mesh size of $8 \times 8 \times 2$, where 8 and 2 are the number of elements in the plane and thickness direction, respectively. Therefore, this mesh size is used for the remaining examples in this study.

Table 1. First four natural frequencies of SCSF Al/ZrO_2-2 square plate

Study	p-order	Mesh	$\bar{\omega}_1$	$\bar{\omega}_2$	$\bar{\omega}_3$	$\bar{\omega}_4$
Present	2	$4 \times 4 \times 2$	3.6811	10.0237	13.6277	19.3464
			(0.1227)*	(0.8993)	(2.0697)	(2.1694)
		$6 \times 6 \times 2$	3.5901	9.3496	12.0275	17.6919
			(0.0317)	(0.2252)	(0.4695)	(0.5149)
		$8 \times 8 \times 2$	3.5688	9.2139	11.6838	17.3441
			(0.0104)	(0.0895)	(0.1258)	(0.1671)
		$10 \times 10 \times 2$	3.5611	9.1684	11.5925	17.2404
			(0.0027)	(0.0440)	(0.0345)	(0.0634)
		$12 \times 12 \times 2$	3.5574	9.1473	11.5599	17.1974
			(0.0010)	(0.0229)	(0.0019)	(0.0204)
	3	$4 \times 4 \times 2$	3.5717	9.2317	11.7667	17.4238
			(0.0133)	(0.1073)	(0.2087)	(0.2468)
		$6 \times 6 \times 2$	3.5638	9.1664	11.5712	17.2249
			(0.0054)	(0.0420)	(0.0132)	(0.0479)
		$8 \times 8 \times 2$	3.5603	9.1466	11.5511	17.1892
			(0.0019)	(0.0222)	(0.0069)	(0.0122)
		$10 \times 10 \times 2$	3.5585	9.1364	11.5461	17.1743
			(0.0001)	(0.0120)	(0.0119)	(0.0027)
[13]			3.5584	9.1244	11.5580	17.1770

* The relative error between the results and exact solutions given by [13]

4.2. Free-vibration behavior of multi-directional FG plates

This subsection presents some examples of the free-vibration behavior of multi-directional FG plates. Five types of plates are examined, they are rectangular plate, square plate with an internal hole, plate with cut-out geometry, circular plate and annular plate. Details about the plane geometry of the plates and the location of origin of coordinate are depicted in Fig. 1. All the plates are assumed to be made from Al/Al_2O_3-2, with the material properties of Al (metal) being $E = 70$ GPa, $\nu = 0.3$, $\rho = 2707$ kg/m^3, and those for Al_2O_3-2 (ceramic) are $E = 380$ GPa, $\nu = 0.3$, $\rho = 3800$ kg/m^3. For rectangular plates, the distribution of ceramic volume fraction follows the law

$$V_c = \left\{\frac{4x}{a}\left(1 - \frac{x}{a}\right)\right\}^{n_1}\left\{\frac{4y}{b}\left(1 - \frac{y}{b}\right)\right\}^{n_2}\left(\frac{z}{h} + \frac{1}{2}\right)^{n_3} \tag{29}$$

For square plates with an internal hole

$$V_c = \left(-\frac{x}{a} + 0.5\right)^{n_1}\left(-\frac{y}{b} + 0.5\right)^{n_2}\left(\frac{z}{h} + \frac{1}{2}\right)^{n_3} \tag{30}$$

For square plates with cut-out geometry

$$V_c = \left(\frac{x}{a}\right)^{n_1}\left(\frac{y}{b}\right)^{n_2}\left(\frac{z}{h}+\frac{1}{2}\right)^{n_3} \tag{31}$$

For circular plates

$$V_c = \left(1-\frac{|r|}{R}\right)^{n_1}\left(\frac{z}{h}+\frac{1}{2}\right)^{n_2} \tag{32}$$

For annular plates

$$V_c = \left(\frac{R_0-|r|}{R_0-R_i}\right)^{n_1}\left(\frac{z}{h}+\frac{1}{2}\right)^{n_2} \tag{33}$$

where $r = \sqrt{x^2+y^2}$ and n_1, n_2, n_3 are the gradient indices that define the variation of material constituent in the plates' volume. For simplification, the following examples are conducted with $n = n_1 = n_2 = n_3$.

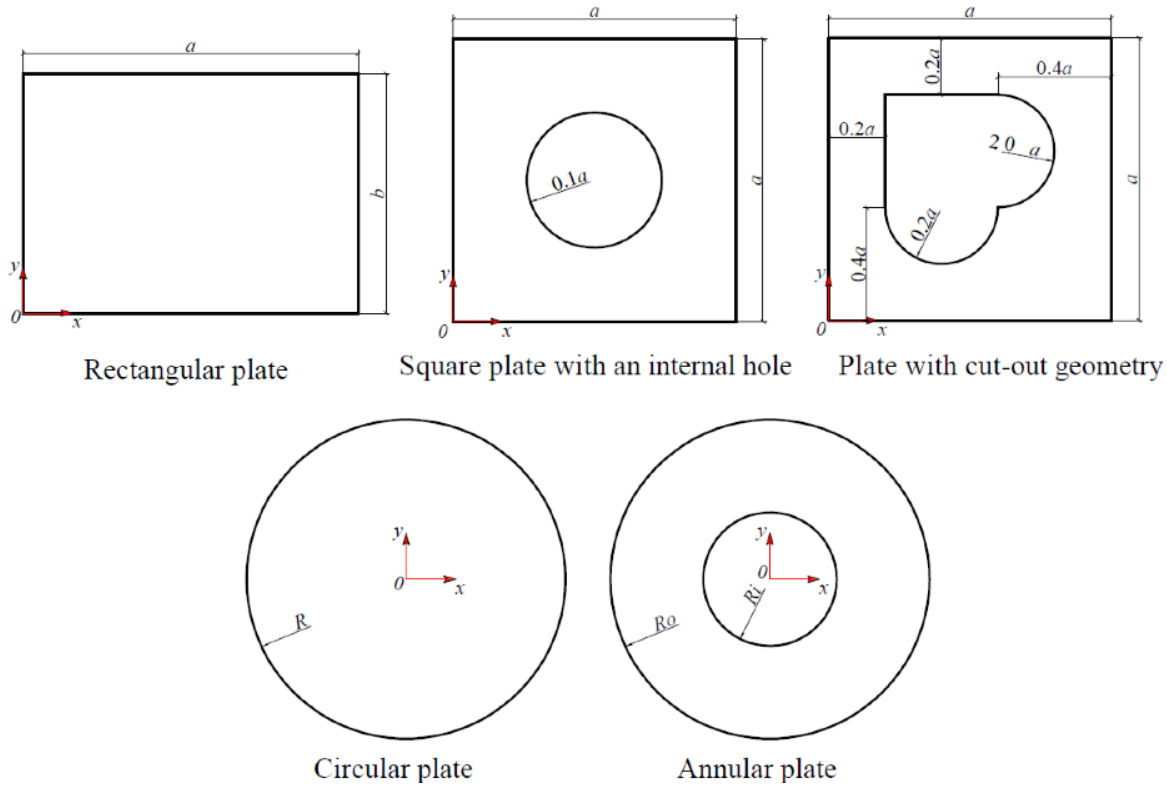

Figure 1. Plane geometries of the plates and locations of the origin of the coordinate system

In Tables 2 to 8, the natural frequencies obtained from different values of gradient indices n. It is noted that the $\bar{\omega} = \omega\left(a^2/h\right)\sqrt{\rho_M/E_M}$ for rectangular plates, square plates with an internal hole, and square plates with cut-out geometry. The non-dimensional frequency for circular plates is $\bar{\omega} = \omega\left(R^2/h\right)\sqrt{\rho_M/E_M}$ and for annular plates is $\bar{\omega} = \omega\left(R_0^2/h\right)\sqrt{\rho_M/E_M}$. The thickness of the plate in those cases is assumed to be $h = a/10$ and $h = R/10$, respectively.

Table 2. First four natural frequencies of SSSS Al_2O_3-2 square plate

	n					
	0	1	2	5	10	100
$\bar{\omega}_1$	5.9219	3.9430	3.5680	3.2946	3.1488	3.0122
$\bar{\omega}_2$	14.6199	9.7323	8.6701	7.8877	7.5824	7.4346
$\bar{\omega}_3$	23.1084	14.9711	13.3670	12.3326	12.0006	11.7526
$\bar{\omega}_4$	28.6674	19.1597	16.9738	15.4453	14.9425	14.5803

Table 3. First four natural frequencies of CCCC Al_2O_3-2 square plate

	n					
	0	1	2	5	10	100
$\bar{\omega}_1$	10.6742	6.6877	6.1573	5.8471	5.6593	5.4296
$\bar{\omega}_2$	21.3315	13.7138	12.4436	11.5707	11.1270	10.8477
$\bar{\omega}_3$	30.8881	19.7475	17.8457	16.5753	16.0799	15.7096
$\bar{\omega}_4$	37.2134	24.3297	21.8867	20.1766	19.4620	18.9272

Table 4. First four natural frequencies of simply supported Al_2O_3-2 circular plate

	n					
	0	1	2	5	10	100
$\bar{\omega}_1$	1.4823	0.9720	0.8646	0.7881	0.7633	0.7538
$\bar{\omega}_2$	4.0955	2.6103	2.3073	2.1228	2.0879	2.0826
$\bar{\omega}_3$	7.3800	4.6399	4.1158	3.8353	3.7768	3.7529
$\bar{\omega}_4$	8.5727	5.5736	4.9378	4.5676	4.4388	4.3594

Table 5. First four natural frequencies of clamped Al_2O_3-2 circular plate

	n					
	0	1	2	5	10	100
$\bar{\omega}_1$	3.0286	1.8231	1.6846	1.5950	1.5578	1.5401
$\bar{\omega}_2$	6.1543	3.7863	3.4341	3.2017	3.1409	3.1296
$\bar{\omega}_3$	9.8520	6.0906	5.4908	5.1333	5.0446	4.9960
$\bar{\omega}_4$	11.1503	7.0793	6.3815	5.9408	5.7757	5.6702

Table 6. First four natural frequencies of clamped Al_2O_3-2 annular plate ($R_i = 0.5R_0$)

	n					
	0	1	2	5	10	100
$\bar{\omega}_1$	5.2065	2.9737	2.7592	2.6853	2.6651	2.6477
$\bar{\omega}_2$	6.2632	3.826	3.5048	3.3288	3.2479	3.1852
$\bar{\omega}_3$	8.8712	5.7519	5.2077	4.8433	4.6613	4.5117
$\bar{\omega}_4$	12.4579	8.2542	7.4261	6.8507	6.5761	6.3361

Table 7. First four natural frequencies of clamped Al_2O_3-2 square plate with a hole

	n					
	0	1	2	5	10	100
$\bar{\omega}_1$	13.4083	7.8037	7.2315	6.8967	6.8272	6.8183
$\bar{\omega}_2$	19.0978	11.2108	10.1927	9.7512	9.7129	9.7116
$\bar{\omega}_3$	28.1772	16.7625	15.2027	14.4725	14.3508	14.3286
$\bar{\omega}_4$	33.3183	19.7439	17.8890	17.0438	16.9483	16.9429

Table 8. First four natural frequencies of clamped Al_2O_3-2 square plate with cut-out geometry

	n					
	0	1	2	5	10	100
$\bar{\omega}_1$	16.0288	9.3676	8.5718	8.1975	8.1543	8.1509
$\bar{\omega}_2$	27.6241	14.6379	14.2045	14.0991	14.0766	14.0473
$\bar{\omega}_3$	27.7661	17.5253	15.9710	14.6033	14.1781	14.1195
$\bar{\omega}_4$	33.6097	19.8190	18.1592	17.3422	17.1327	17.0911

As presented in Tables 2 to 8, the natural frequencies of the plates decrease with the increase of gradient index n. This is due to the increase of metal constituent in the volume of the plate, which tends to reduce to stiffness and consequently reduce the natural frequencies of the structures. It is noted that the results presented in Tables 2 to 6 can be considered as benchmark results for other work related to multi-directional FG plates in the future. For illustration purpose, the first four vibration mode shapes are also depicted in Figs. 2 to 6.

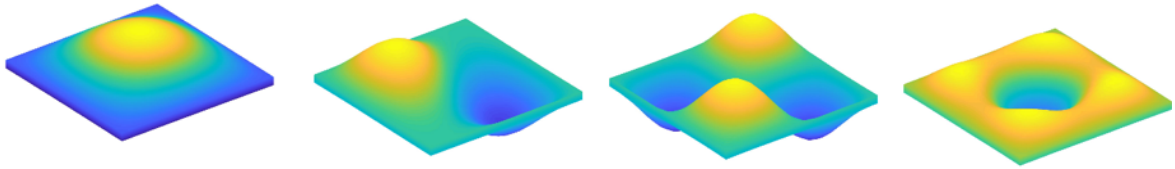

Figure 2. First four free-vibration mode shapes of a SSSS square plate

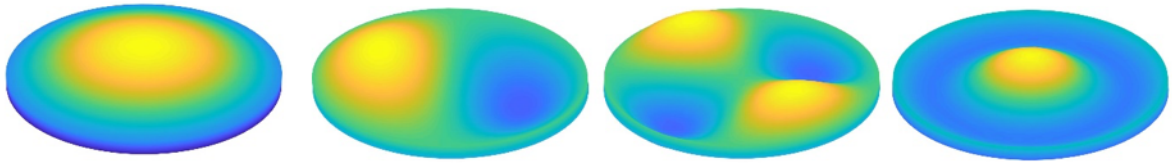

Figure 3. First four free-vibration mode shapes of a simply supported circular plate

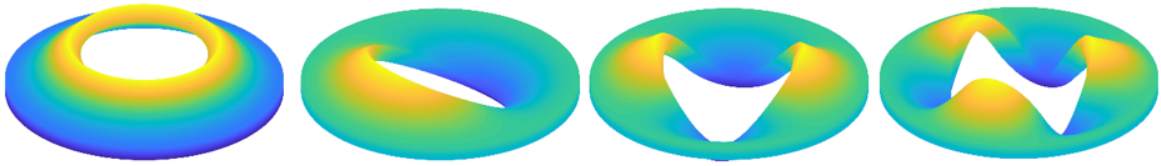

Figure 4. First four free-vibration mode shapes of a simply supported annular plate

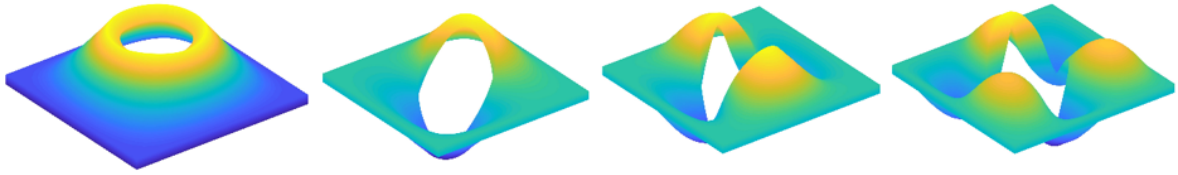

Figure 5. First four free-vibration mode shapes of a SSSS square plate with an internal hole

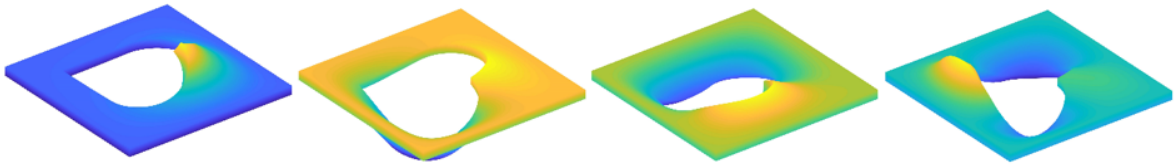

Figure 6. First four free-vibration mode shapes of a simply supported square plate with cut-out geometry

5. Conclusions

In this study, the free-vibration analysis of multi-directional FG plates is investigated based on the framework of 3D elasticity analysis, whereby the governing equation is developed based on the theory of infinitesimal elasticity theory. The IGA approach with NURBS basis functions are employed as a discretization tool to solve the problems. A numerical example retrieved from literature is revisited to verify the accuracy of the proposed approach. In addition, various examples are presented to show the efficiency of the proposed approach in analyzing the response of multi-directional FG plates. The results presented in this paper could be used as benchmark results for further investigation.

References

[1] Reddy, J. N. (2003). *Mechanics of laminated composite plates and shells: theory and analysis*. Second edition, CRC Press.

[2] Koizumi, M. (1993). The concept of FGM. *Ceramic Transactions, Functionally Gradient Materials*, 34: 3–10.

[3] Koizumi, M. (1997). FGM activities in Japan. *Composites Part B: Engineering*, 28(1-2):1–4.

[4] Thai, H.-T., Kim, S.-E. (2015). A review of theories for the modeling and analysis of functionally graded plates and shells. *Composite Structures*, 128:70–86.

[5] Nemat-Alla, M. (2003). Reduction of thermal stresses by developing two-dimensional functionally graded materials. *International Journal of Solids and Structures*, 40(26):7339–7356.

[6] Lü, C. F., Lim, C. W., Chen, W. Q. (2009). Semi-analytical analysis for multi-directional functionally graded plates: 3-D elasticity solutions. *International Journal for Numerical Methods in Engineering*, 79 (1):25–44.

[7] Nie, G., Zhong, Z. (2010). Dynamic analysis of multi-directional functionally graded annular plates. *Applied Mathematical Modelling*, 34(3):608–616.

[8] Shariyat, M., Alipour, M. M. (2011). Differential transform vibration and modal stress analyses of circular plates made of two-directional functionally graded materials resting on elastic foundations. *Archive of Applied Mechanics*, 81(9):1289–1306.

[9] Nguyen, T.-T., Lee, J. (2018). Flexural-torsional vibration and buckling of thin-walled bi-directional functionally graded beams. *Composites Part B: Engineering*, 154:351–362.

[10] Nguyen, T.-T., Lee, J. (2018). Interactive geometric interpretation and static analysis of thin-walled bi-directional functionally graded beams. *Composite Structures*, 191:1–11.

[11] Wang, X., Yuan, Z., Jin, C. (2019). 3D free vibration analysis of multi-directional FGM parallelepipeds using the quadrature element method. *Applied Mathematical Modelling*, 68:383–404.

[12] Hughes, T. J. R., Cottrell, J. A., Bazilevs, Y. (2005). Isogeometric analysis: CAD, finite elements, NURBS, exact geometry and mesh refinement. *Computer Methods in Applied Mechanics and Engineering*, 194(39-41):4135–4195.

[13] Nguyen, V. P., Anitescu, C., Bordas, S. P. A., Rabczuk, T. (2015). Isogeometric analysis: an overview and computer implementation aspects. *Mathematics and Computers in Simulation*, 117:89–116.

[14] Nguyen, K. D., Nguyen-Xuan, H. (2015). An isogeometric finite element approach for three-dimensional static and dynamic analysis of functionally graded material plate structures. *Composite Structures*, 132: 423–439.

[15] Lieu, Q. X., Lee, D., Kang, J., Lee, J. (2018). NURBS-based modeling and analysis for free vibration and buckling problems of in-plane bi-directional functionally graded plates. *Mechanics of Advanced Materials and Structures*, 1–17.

[16] Lieu, Q. X., Lee, S., Kang, J., Lee, J. (2018). Bending and free vibration analyses of in-plane bi-directional functionally graded plates with variable thickness using isogeometric analysis. *Composite Structures*, 192: 434–451.

[17] Lieu, Q. X., Lee, J. (2019). A reliability-based optimization approach for material and thickness composition of multidirectional functionally graded plates. *Composites Part B: Engineering*, 164:599–611.

[18] Lieu, Q. X., Lee, J. (2019). An isogeometric multimesh design approach for size and shape optimization of multidirectional functionally graded plates. *Computer Methods in Applied Mechanics and Engineering*, 343:407–437.

[19] Hosseini-Hashemi, S., Fadaee, M., Atashipour, S. R. (2011). A new exact analytical approach for free vibration of Reissner–Mindlin functionally graded rectangular plates. *International Journal of Mechanical Sciences*, 53(1):11–22.